Deformation and Aspect Ratio of Bubbles Continuously Rising in Shear-Thinning Fluids

Sun, Wanpeng; Zhu, Chunying*[+]; Fu, Taotao; Ma, Youguang

State Key Laboratory of Chemical Engineering, School of Chemical Engineering and Technology, Tianjin University, Tianjin 300072, P.R. CHINA

ABSTRACT: *The shape deformation of three bubbles with equilateral triangle arrangement continuously rising in shear-thinning non-Newtonian fluids was numerically investigated using the three-dimensional volume of fluid method (3D-VOF). The shape deformation of three continuously rising bubbles was compared with that of a single bubble under consistent operations to analyze the effect of interaction between bubbles. The influences of bubble diameter, initial bubble distance, bubble formation frequency, and liquid rheological property on the aspect ratio of the bubble were investigated. The results indicate that the aspect ratio of the bubble for multi-bubble systems with greater bubble diameter, initial bubble distance, and more intense shear-thinning effect of the liquid decreases and the shape of the bubble deforms flatter. However, as the bubble formation frequency increases, the deformation of the bubble weakens, and the bubble aspect ratio increases. In comparison with the single bubble rising freely, the aspect ratio of the bubble for the multi-bubble systems is larger. Moreover, a modified model of the aspect ratio of the bubble was proposed by considering the interaction between bubbles for the multi-bubble system.*

KEYWORDS: *Bubble, Bubble deformation; Aspect ratio; Shear-thinning fluid; Bubble column.*

INTRODUCTION

The gas-liquid two-phase flow is frequently employed in industrial applications such as the petrochemical, pharmaceutical, and food industries, in which the gas phase usually dispersed into the liquid phase to form the bubbly flow [1-4]. The heat transfer, mass transfer, and chemical reactions during the bubble rising is closely related to the interfacial area and contacting time between two phases [5, 6]. The qualitative analysis and predicting models of the movement and shape variation for bubbly flows has been one of the research hotspots due to the complicated interaction between bubbles and the surrounding fluid [7-12].

The bubble deformation, which directly depends on the bubble size, bubble rising motion, and liquid property is believed to be of vital importance in practical applications [13-15]. The various steady shape of bubbles rising in viscous liquids had been investigated in the work of *Bhaga* and *Weber* (1981), and typical bubbles such as spherical, oblate ellipsoidal, spherical cap and skirted, were determined [16]. The bubble deformation in glycerol-water solutions was analyzed in the range of (Re,We) = [1,100] × [0,5] by *Raymond* and *Rosant* (2000) [17], the results showed that the aspect ratio of spheroid shape decreased with bubble diameter and tended to a constant 0.24 corresponding to a spherical-cap bubble.

** To whom correspondence should be addressed.*
+ E-mail: zhchy971@tju.edu.cn
1021-9986/2021/2/667-681 15/$/6.05

Legendre et al. (2012) collected comprehensive data from the literature and experiments. Considering the effect of the bubble diameter and the liquid viscosity on the bubble deformation, an expression to describe the bubble deformation using the Morton and Weber number was proposed [18]. *Tripathi et al.* (2015) studied the dynamics of bubble rising in a Bingham fluid with weak surface tension, results showed that the bubble aspect ratio exhibitsed oscillations about unity, and the amplitude and wavelength increased with the increase of yield stress and the decrease of surface tension [19]. *Premlata et al.* (2017) numerically studied the rising motion of an air bubble in the non-Newtonian fluids, and found that the rise velocity of bubbles increased while the deformation of the bubble weakened with the increase of the shear thinning effect of the liquid [20]. Moreover, *Xu et al.* (2017) investigated experimentlly the rising behavior of single air bubbles in non-Newtonian liquid, and proposed that the deformation could change the trajectories of rising bubbles and bubble hydrodynamics [21]. *Pang and Lu* (2018) studied the rise behavior and deformation of single bubble in the shear-thinning non-Newtonian fluid by using VOF method, the results showed that the bubble deformation strengthened and the circulating region in the bubble wake magnified with decreasing rheological index [22].

The shape variation of the bubble was usually characterized by aspect ratio E in the literature, which is the ratio of the bubble maximum diameter in the vertical direction to the maximum diameter in horizontial direction [23]. Models of aspect ratio E was frequently correlated through Reynolds number (Re), Eötvös number (Eo) and Weber number (We) [22, 24]. Moreover, *Chen et al.* (1999) found that the aspect ratio of the bubble could be characterized by the Reynolds number (Re), the Bond number (Bo), the density ratio, and the viscosity ratio [25]. The motion and deformation of vapour bubbles in one-component systems were studied experimentally by *Celata et al.* (1999), and a satisfactory prediction of bubble shape was proposed based on the *Taylor* and *Acrivos* model (1964) [26, 27]. *Kelbaliyev and Ceylan* (2004) derived a new correlation of aspect ratio in terms of the dimensionless numbers such as Reynolds number (Re), Morton number (Mo), and Weber number (We), the comparison between calculated values and the experimental data showed a good consistency [24]. *Lalanne et al.* (2015) investigated the moderate non-linear shape oscillations of a rising bubble by means of experiment and numerical simulation [28]. However, the deformation of the bubble affected by mutual factors, such as the viscous force, inertia force, and surface force, would be significantly complicated for the multi-bubble system in comparison with a single bubble rising in stagnant liquid [29-31]. Therefore, the understanding of the deformation and aspect ratio of the bubble for the multi-bubble systems in complex fluids is still lacking so far.

In this work, the deformation of bubbles continuously rising with equilateral triangle arrangement was simulated by 3D-VOF method in shear-thinning non-Newtonian fluids. The influences of bubble diameter (d), initial bubble distance (S), bubble formation frequency (f) and liquid rheological property on the deformation and aspect ratio E of bubbles were investigated, respectively. Accordingly, the deformation and aspect ratio E of bubbles for multi-bubble systems were compared with a single bubble to analyze the effect of interaction between bubble. A new correlation of aspect ratio E was proposed with satisfactory accuracy for the multi-bubble system in shear-thinning non-Newtonian fluids.

THEORITICAL SECTION

Numerical simulations were employed to investigate the deformation and motion of three bubbles with equilateral triangle arrangement continuously rising in shear-thinning non-Newtonian fluids. The Navier-Stokes equations for multi-phases were solved adopting the Volume of Fluid (VOF) and Continuum Surface Force (CSF) by ANSYS Fluent. The main underlying assumptions of the simulation were (1) the two fluids were incompressible, (2) the gas-liquid flow was in laminar state and isothermal. The continuity and Navier-Stokes equations could be written as:

$$\nabla \cdot \mathrm{u} = 0 \tag{1}$$

$$\frac{\partial}{\partial \mathrm{t}}(\rho \mathrm{u}) + \nabla \cdot (\rho \mathrm{uu}) = -\nabla \mathrm{p} + \nabla \cdot (2\mu \mathrm{D}) + \mathrm{F_s} + \rho \mathrm{g} \tag{2}$$

Where u represents the velocity vector, D represents the stress tensor, p represents the pressure, F_s represents the body force introduced by the surface tension. The volume fraction (Q) was defined as the fraction of the liquid inside a control cell, in which the value of Q adopts 0 for a pure gas cell: 1 for a pure liquid cell and between 0

and 1 for an interface of gas and liquid in the cell. The density (ρ) and viscosity (μ) of the mixed fluid were computed as the averages of the two phases with the volume fraction Q :

$$\rho = \rho_l Q + \rho_g (1 - Q) \tag{3}$$

$$\mu = \mu_l Q + \mu_g (1 - Q) \tag{4}$$

The viscosity of the shear-thinning fluid is calculated by the power-law model [32]:

$$\mu_l = K\gamma^{n-1} \tag{5}$$

Where K and n are the consistency coefficient and flow index, respectively. The shear-thinning effect of non-Newtonian fluid could be reflected by flow index n, γ represents the shear rate. The surface tension force term F_s in Eq. (2) was calculated as a volumetric force with the Continuum Surface Force (CSF) model proposed by *Brackbill et al.* (1992) [33]:

$$F_s = \sigma \frac{\rho \kappa \nabla Q_g}{0.5(\rho_g + \rho_l)} \tag{6}$$

Where Q_g is the volume fraction of the gas phase. The solution of the surface curvature κ was obtained by the divergence of the unit normal vector n to the interface as following equation:

$$\kappa = \frac{1}{|n|}\left[\frac{n}{|n|}\cdot\nabla|n| - (\nabla \cdot n)\right] \tag{7}$$

$$n = \nabla Q_g \tag{8}$$

The volume fraction Q was solved by piecewise linear interface calculation (PLIC). For pressure-velocity coupling, the Pressure Implicit with Splitting of Operators (PISO) scheme was employed. The pressure staggering option (PRESTO) and first-order upwind scheme were used for the discretization of the pressure interpolation scheme and momentum equation. The cubic computational domain for 3-D simulation with dimension of 40 mm × 40 mm × 50 mm was constructed with structured mesh. The surfaces of the side and bottom of the computational domain were considered as no-slip walls, and the upper face was assigned as the pressure outlet boundary condition.

The rising motion of the bubble was simulated by patching bubbles with a fixed time interval into the domain. The three spherical bubbles, with equilateral triangle arrangement in X-Y plane, were simultaneously placed 1 mm above the bottom in Z direction. The shear-thinning non-Newtonian fluid was chosen as the primary phase, and then it was driven to flow by the bubble motion until achieved steady flow pattern. The pressure above the liquid column for the open system was 101.325 kPa; and the temperature was 298.15 K; the time step was 1.0×10^{-5} s. Consistent initial operating conditions were adopted for a single bubble and multiple bubbles.

RESULTS AND DISCUSSION

Validation

Numerical simulation of one group of three bubbles with equilateral triangle arrangement rising freely in stagnant liquid were carried out to observe the effect of mesh size on the motion and deformation of the bubble. The diameters (d) of bubble for the minimum and maximum resolution conditions were 4 mm and 8 mm, and the initial bubble distances (S) were 7.2 mm and 14.4 mm, respectively. The initial parameters of the liquid phase for the grid refinement test were flow index (n) = 0.89, consistency coefficient (K) = 0.072 Pa·s^n, density (ρ) = 998.2 kg/m^3 and surface tension (σ) = 0.060 N/m, respectively. Fig. 1 displays the shape, aspect ratio and average rising velocity of three bubbles. The shape of the deformed bubble is characterized by the aspect ratio, E, which is the ratio of the maximum vertical dimension to the maximum horizontal dimension.

$$E = \frac{d_v}{d_h} \tag{9}$$

It could be found from Fig. 1(a) that the shape of the bubble with a diameter of 4 mm at a mesh size of 0.4 mm is slightly rough, which is visibly different from the bubble shape at other mesh sizes. Furthermore, with the decrease of mesh size from 0.35 mm to 0.25 mm, deviations of the bubble rising velocity and aspect ratio reduce gradually, as shown in Figs. 1(c), (e). The consistent evolution of the shape, aspect ratio and rising velocity of the bubble could also be observed for the largest bubbles from Figs. 1(b), (d), (f). Furthermore, the negligible difference could be clearly found for grid sizes of 0.3 mm and 0.25 mm. Although the bubble dynamics and liquid film between

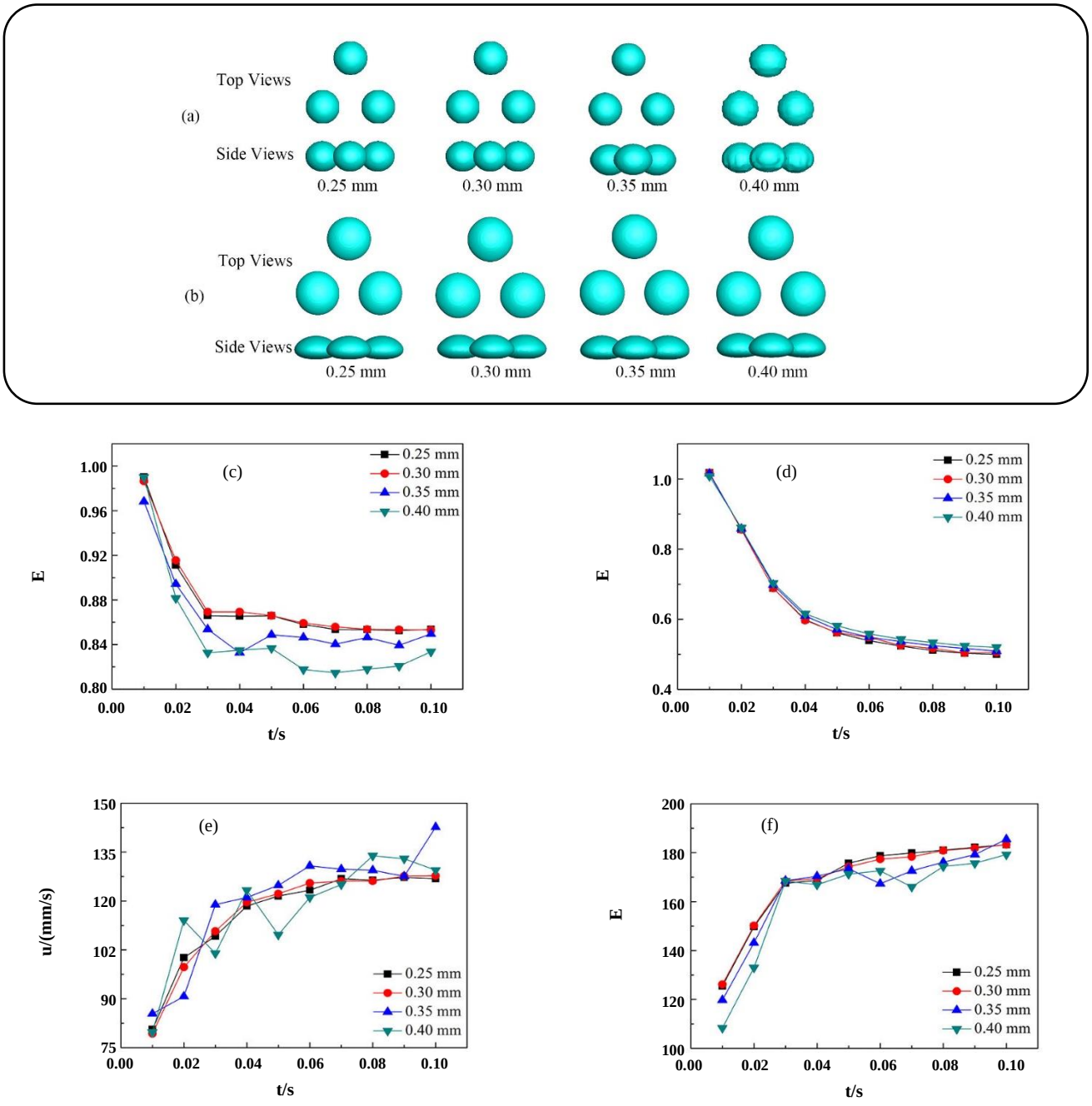

Fig. 1: Effect of the mesh size on the shape, aspect ratio and rising velocity of three bubbles with equilateral triangle arrangement. Shapes at 0.07 s with different diameters (a) d = 4 mm; (b) d = 8 mm. The aspect ratio of the bubble with different diameters (c) d = 4 mm; (d) d = 8 mm. The rising velocity of the bubble with different diameters (e) d = 4 mm; (f) d = 8 mm. Mesh size: 0.25 mm, 0.3 mm, 0.35 mm, 0.4 mm.

two bubbles have been investigated with the grid size of 0.5 mm in the literature, it was certified to be rather coarse for present study due to the different simulation systems [34-36]. According to the grid independent validation, a mesh with the grid size of 0.30 mm was adopted in the simulation jointly balancing the simulation accuracy and computational power.

In order to validate the reliability of the numerical method, processes of the parallel rise of two groups of pair bubbles in shear-thinning fluids were simulated and

Table 2: Comparisons of bubble dynamics between the experimental values and simulation results.

	Bubble with coalescence		Bubble without coalescence	
	Experimental results	Simulative results	Experimental results	Simulative results
u_t (mm·s^{-1})	204.23	202.54	190.31	193.25
E	0.453	0.449	0.521	0.535
Re	29.38	30.23	16.27	16.55

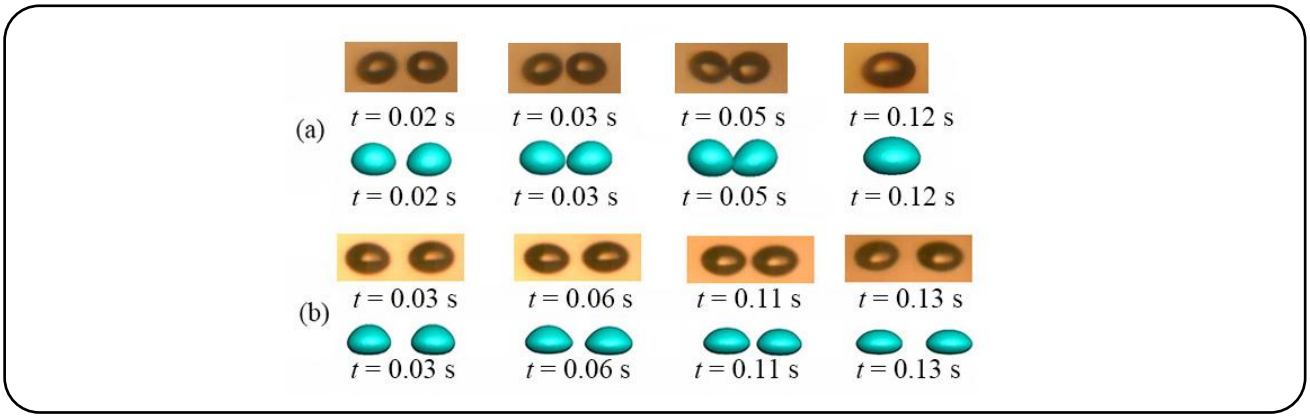

Fig. 2: The movement of a pair of bubbles rising side by side. (a) experimental and simulation results for bubbles with coalescence (S = 6 mm, n = 0.89, K = 0.072 Pa·s^n); (b) experimental and simulation results for bubbles without coalescence (S = 9 mm, n = 0.89, K = 0.072 Pa·s^n).

compared with experimental results. The experimental apparatus was the same as that in our previous work [37]. The flow index, consistency coefficient, density and surface tension of the liquid were 0.89, 0.072 Pa·s^n, 1000.17 kg·m^{-3} and 0.058 N·m^{-1} for experimental conditions, respectively. The bubble diameter was 4.9 mm, and the initial bubble distances were 6 mm for bubbles with coalescence, while 9 mm for bubbles without coalescence, respectively. The rising motion of bubbles is shown in Fig. 2. The steady rising velocity u_t, the aspect ratio *E* and the bubble Reynolds number *Re* were obtained and compared with the experimental values as depicted in Table 1. For bubbles with horizontal coalescence, the simulated results of the deformation and rising velocity of bubbles in the coalescence process agree well with the experimental results as shown in Fig. 2(a), and relative deviation of the Reynolds number (2.9%) for bubbles reaching steady after coalescence is ignorable. As indicated in Fig. 2(b), bubbles without coalescence approach until the critical distance in horizontal direction, then depart. The shape and distance of bubbles in the rising process show nearly identical results. Finally, the aforementioned comparison confirms that the numerical method is reliable and conducts satisfactory accuracy in the present investigation.

The deformation of bubbles

The motion behavior of a single bubble and multiple bubbles with equilateral triangle arrangement rising freely in stagnant shear-thinning fluids were simulated. In terms of the multi-bubble systems with groups of three bubbles continuously rising in the liquid, the stagnant liquid flows due to the squeezing action of bubbles after the entrance of the first bubble group. The liquid flow is intensified and gradually trends stability after the entrance of subsequent bubble groups. The evolutions of the aspect ratio and rising velocity of the bubble for a series of bubble groups with time *t* were shown in Fig. 3. It can be seen that the aspect ratio and rising velocity of bubbles have trended to the constant before they reached the top of the domain, indicating the domain is large enough to study the deformation of bubble in this work. Furthermore, the deviation of the aspect ratio and rising velocity between the third bubble cluster and subsequent clusters is very

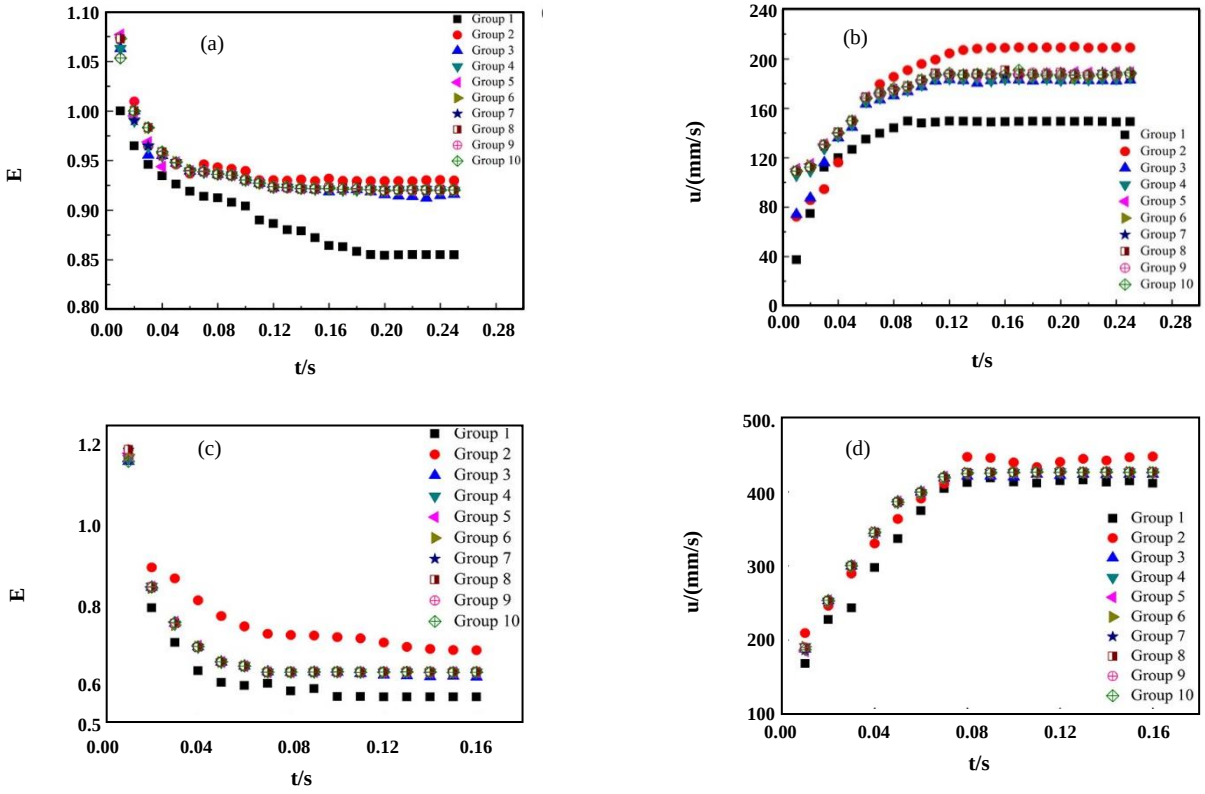

Fig. 3: Evolution of the aspect ratio and rising velocity of the series of bubble clusters. (a) aspect ratio of the bubble with diameter 4 mm; (b) rising velocity of the bubble with diameter 4 mm; (c) aspect ratio of the bubble with diameter 8 mm; (d) rising velocity of the bubble with diameter 8 mm. (S* = 2.0, f = 16 Hz, n = 0.89, K = 0.072 Pa·s^n).

small, indicating the motion and deformation of bubbles after the third bubble cluster could be considered as stable. Consequently, the entrance of the fifth cluster of bubbles was defined as the starting moment, and the rising process of the fifth cluster of bubbles from the entrance to the departure was focused on.

The bubble clusters with different diameters d (4 mm, 5 mm, 6 mm, 7 mm and 8 mm), bubble formation frequencies f (10 Hz, 16 Hz and 20 Hz), and flow indexes n (0.49, 0.69 and 0.89) were simulated to investigate the influence of the interaction between bubbles on the motion and deformation of bubbles. The dimensionless initial bubble distance S^* (1.2, 1.4, 1.6, 1.8 and 2.0), which is the ratio of the bubble distance S and equivalent bubble diameter d_e, was chosen to explore the influence of bubble distance on the bubble dynamics.

Fig. 4 shows the schematic diagrams of typical bubble shapes and the comparison with the literature [17]. The typical bubble shape includes sphere (4 mm), ellipsoid (5 mm, 6 mm) and spherical cap (5 mm, 6 mm) in this simulation. The deformation of bubbles in the rising process is shown in Fig. 5. The vertical diameter of the rising bubble decreases gradually, while the horizontal diameter increases until stabilization.

The effect of bubble diameter and initial bubble distance

The rising velocity, path and deformation of a single bubble are closely related to the variation of the initial bubble diameter and rheological property of the liquid in the stagnant liquid [38-40]. While the deformation of bubbles in multi-bubble systems would be more complicated in comparison with the single bubble due to the influences of interaction between bubbles and surrounding liquid due to the coupling of the velocity and viscosity fields around the bubble. Fig. 6 shows the effects of the bubble diameter and initial bubble distance on the aspect ratio of the bubble.

For the multi-bubble system without coalescence, the bubble approaches in horizontal direction until the critical distance, and then departs; the rising velocity of bubble

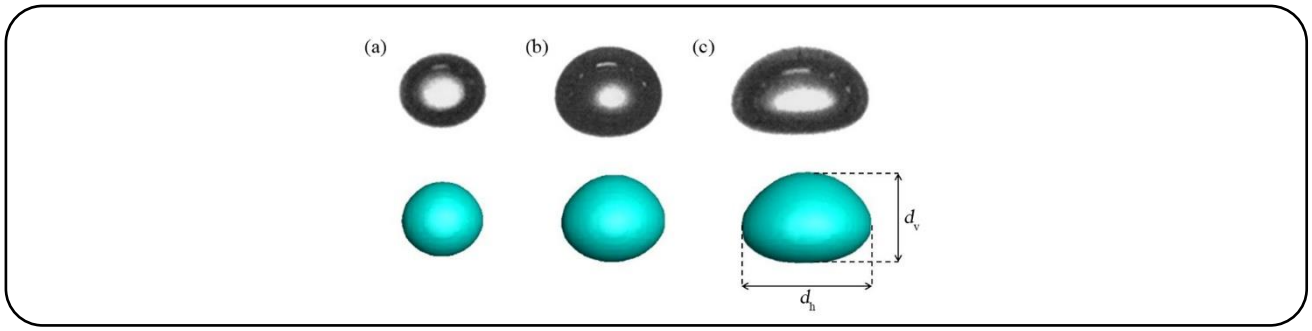

Fig. 4: Schematic diagrams of typical bubble shapes. Experimental photographs are obtained from the literature [17]. (a) E = 0.93, sphere; (b) E = 0.84, ellipsoid; (c) E = 0.66, spherical cap. (S* = 2.0, f = 16 Hz, n = 0.89, K = 0.072 Pa·s^n).

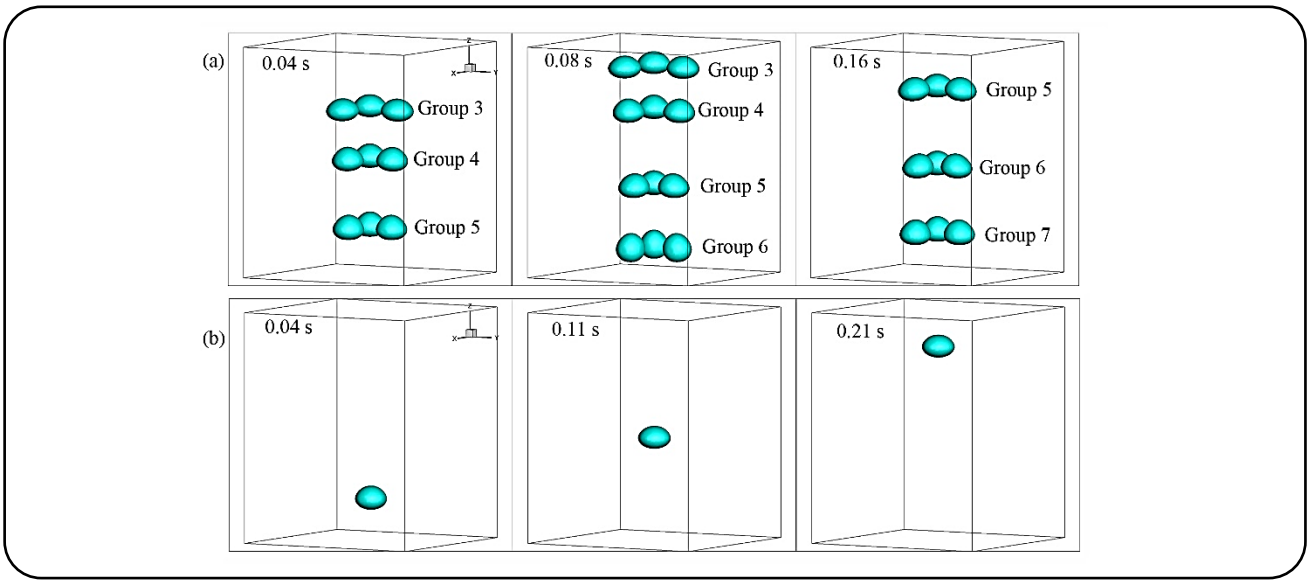

Fig. 5: Schematic representation of the bubble motion for two cases under the same condition. (a) multi-bubble system (S* = 1.8, f = 16 Hz); (b) a single bubble. (d = 6 mm, n = 0.89, K = 0.072 Pa·s^n).

increases along with the symmetry-axis, finally achieves steady. The aspect ratio of the bubble decreases with increasing bubble diameter, and the similar evolution of the aspect ratio could be found for the single bubble system as shown in Fig. 6. The aspect ratio of the single bubble is smaller than that of the multi-bubble system with the same diameter, while the aspect ratio of bubbles for the multi-bubble system decreases with the increase of initial distance. Furthermore, the change rate of the aspect ratio to bubble diameter for the single bubble system is 1.1 times higher than that of the multi-bubble system, demonstrating significant influence of the interaction on the deformation of the bubble.

The buoyancy force, drag force, inertia force and surface tension force are the important factors controlling the bubble deformation. The Reynolds number, which is the ratio of the drag force and the inertia force, could be calculated as following:

$$Re = \frac{\rho_l d_e^n u_b^{2-n}}{K} \tag{10}$$

where d_e, u_b represent the bubble equivalent diameter and terminal rising velocity; ρ_l, n, K are the liquid density, flow index and consistency coefficient, respectively.

For the bubble rising in the viscous fluid, the surface tension force maintains the bubble as a sphere, and would hinder the deformation of bubbles, leading to an analogous performance as the rigid sphere. The same evolution of the shape for a gas bubble rising in water-glycerin solutions was also found in the work [18]. For the multi-bubble system, the wake effect of the leading bubble cluster intensifies with the increase of the bubble diameter,

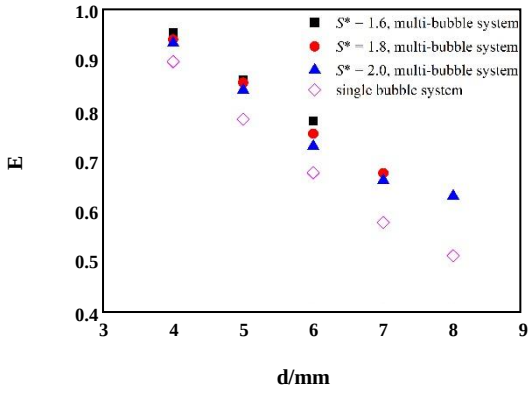

Fig. 6: Effects of the bubble diameter and initial bubble distance on the bubble deformation. (f = 16 Hz for multi-bubble system, n = 0.89, K = 0.072 Pa·s^n).

leading to the decrease of liquid viscosity around the trailing bubble cluster as shown in Fig. 7(a). Correspondingly, the viscous force on the trailing bubbles would decrease, while the rising velocity of the trailing bubble cluster increases (Fig. 7(c)), which enhances the inertia force. Since the viscous and inertia forces intensify the axial compression on the bubble, it was found that the bubble expanded in radial direction with increasing the bubble diameter. Accordingly, the deformation of the bubble for the multi-bubble system intensifies, while the aspect ratio declines with the increase of the bubble diameter.

The liquid between the trailing bubbles would hinder the radial approach of bubbles, and squeeze them in the radial direction. With the reduction of the initial bubble distance, the liquid zone would also decrease, the squeezing action of liquid on bubbles accordingly enhances when bubbles gradually approach, leading to the shrinkage of the bubble in radial direction. Simultaneously, the viscosity of liquid on bubbles increases slightly as displayed in Fig. 7(b), resulting in an increase of the viscous resistance to the rising bubbles, while the rising velocity and inertial force for bubbles reduce. Finally, bubbles expand in axial direction. Therefore, the aspect ratio of the bubble for the multi-bubble systems increases with the decrease of the initial bubble distance (Fig. 6).

The effect of bubble formation frequency

For multi-bubble systems continuously rising with different formation frequency, the intervals of space and time between two groups of bubble clusters would influence the bubble aspect ratio. Fig. 8 shows the effect of the bubble formation frequency on the bubble aspect ratio.

For bubbles continuously rising in the shear-thinning fluids, the viscosity of the liquid around bubbles reduces due to the shear stress by the motion of the leading bubbles as shown in Fig. 9. With the decrease of bubble formation frequency, the axial interval between the leading and trailing bubble clusters enlarges, thus the wake effect on the trailing bubble cluster weakens [41]. Inversely, the spatial interval between the leading and the trailing bubble clusters decreases for larger bubble formation frequency, the wake effect of the leading bubble cluster strengthens accordingly, and the suction effect on the trailing bubbles intensifies. The trailing bubbles are stretched along vertical direction, leading to the increase of bubble aspect ratio [42, 43]. On the other hand, the horizontal interval between bubbles decreases with the raise of bubble formation frequency (Fig. 9). Consequently, the compression of the liquid on bubbles in horizontal direction intensifies, as a result, the bubbles radially shrink. Finally, the bubble aspect ratio increases with the bubble formation frequency (Fig. 8).

The effect of the shear-thinning effect of the liquid

The viscosity of the liquid would decrease at the same shear rate with the decrease of the flow index for the shear-thinning fluid. The influence of the shear thinning effect of the non-Newtonian fluid on the bubble deformation was displayed in Fig. 10.

As shown in Fig. 11, the wake effect would be weaker for the liquid with high flow index for the shear-thinning fluid, and accordingly higher viscosity could be found. The viscous force on the rising bubbles enhances, enlarging the stretching for bubbles in vertical direction. Moreover, the radial compression of liquid on bubble would be strengthened with the increase of liquid viscosity in the radial direction. Therefore, the aspect ratio of the steady bubble increases for larger flow index due to the axial expansion and radial shrinkage.

Model of bubble aspect ratio

Etensive studies have been conducted in the past decades and focused on the correlation between the aspect ratio and the dimensionless parameters, such as the Eötvös

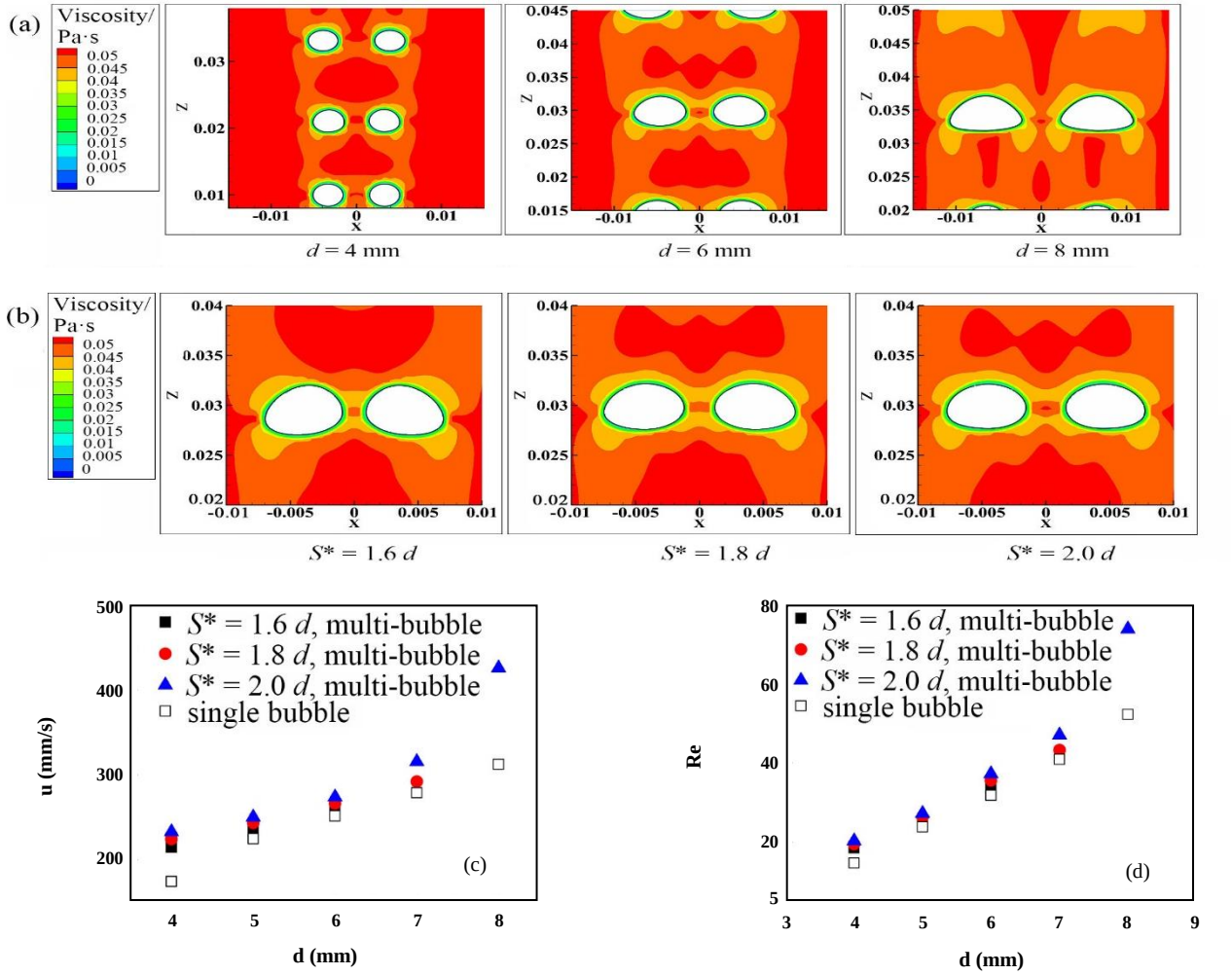

Fig.7: The dynamics of trailing bubbles. (a) the liquid viscosity fields around bubbles at t = 0.12 s and Y = - 0.002 m (S* = 2.0, f = 16 Hz, n = 0.89, K = 0.072 Pa·s^n); (b) liquid viscosity fields around bubbles at t = 0.12 s and Y = - 0.002 m (d = 6 mm, f = 16 Hz, n = 0.89, K = 0.072 Pa·s^n); (c) bubble rising velocity (f = 16 Hz, n = 0.89, K = 0.072 Pa·s^n); (d) bubble Reynolds number (f = 16 Hz, n = 0.89, K = 0.072 Pa·s^n). The black profile lines represent the interface location of bubbles.

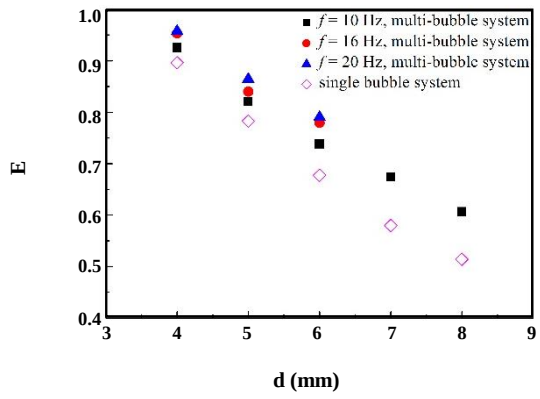

Fig.8: Effects of the bubble formation frequency on the bubble deformation for a single bubble and multi-bubbles (S* = 1.6, n = 0.89, K = 0.072 Pa·s^n).

number (*Eo*), Reynolds number (*Re*), Weber number (*We*) and Tadaki number (*Ta*) [14, 23, 24, 44, 45]. Accordingly, a number of models of the bubble deformation, which could provide the basis to study the terminal rising velocity, drag coefficient and lift coefficient of the bubble, were proposed [39, 46].

The rise of a gas bubble in the viscous liquid was investigated by *Moore* (1959) on the basis of results in the literature [23]. They showed the correlation of aspect ratio of an oblate spherical bubble with the Weber number *We*:

$$E = \frac{1}{1 + \frac{9}{64} We} \quad (11)$$

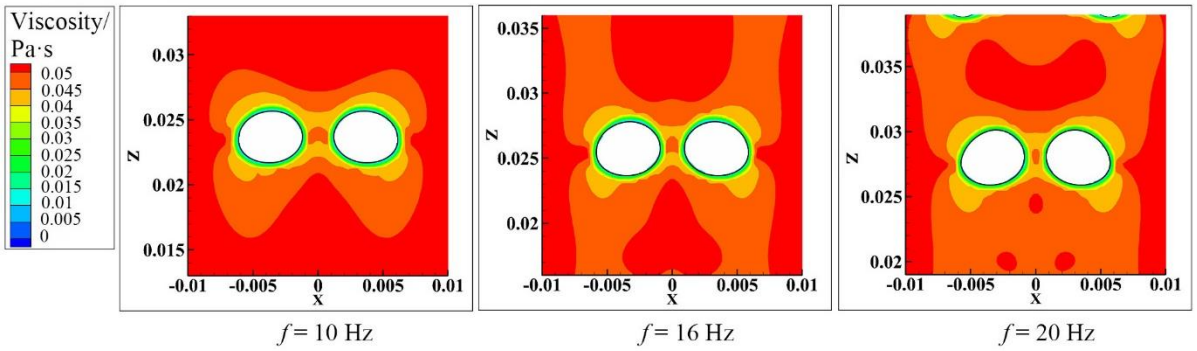

Fig.9: The liquid viscosity around bubbles for different bubble formation frequencies at t = 0.12 s and Y = - 0.0023 m. The black profile lines represent the interface location of bubbles, d = 5 mm, S* = 1.6, n = 0.89, K = 0.072 Pa·s^n.

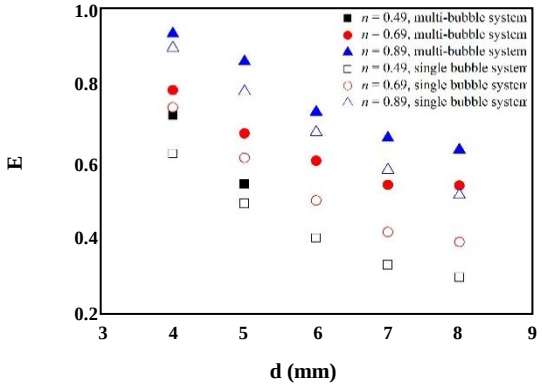

Fig. 10: The effect of the liquid flow index on the bubble deformation (S* = 2.0 and f = 16 Hz for multi-bubble system, K = 0.072 Pa·s^n).

$$We = \frac{\rho_l u_t^2 d_e}{\sigma_l} \tag{12}$$

where u_t repersents the terminal rising velocity of the bubble.

Tadaki and Maeda (1961) considered that the aspect ratio E was a function of the Reynolds number Re and the Morton number Mo in the liquids ($Mo < 2.5\times10^{-4}$) [47]. They introduced a new dimensionless number, Tadaki number Ta, to correlate the aspect ratio E:

$$E^{1/3} = \begin{cases} 1 & Ta < 2 \\ 1.14Ta^{-0.176} & 2 < Ta < 6 \\ 1.36Ta^{-0.28} & 6 < Ta < 16.5 \\ 0.62 & 16.5 < Ta \end{cases} \tag{13}$$

$$Mo = \frac{g\mu_l^4}{\sigma_l^3 \rho_l} \tag{14}$$

$$Ta = ReMo^{0.23} \tag{15}$$

Then, the above correlation of the aspect ratio was modified by *Vakhrushev and Efremov* (1970) [48]:

$$E = \begin{cases} 1 & Ta < Ta_1 \\ \left\{c_1 + c_2 \tanh\left[c_3\left(c_4 - \log_{10}^{Ta}\right)\right]\right\}^m & Ta_1 \le Ta < Ta_2 \\ c_5 & Ta_2 \le Ta \end{cases} \tag{16}$$

Fan and Tsuchiya (1990) developed the above model of *Vakhrushev and Efremov* (1970) based on the analysis of bubble deformation [44]:

$$E = \begin{cases} 1 & Ta < 1.0 \\ \left\{0.81 + 0.20\tanh\left[2.0\left(0.8 - \log_{10}^{Ta}\right)\right]\right\}^3 & 1.0 < Ta < 40 \\ 0.24 & 40 < Ta \end{cases} \tag{17}$$

An equation of aspect ratio E of the bubble ($0.5 < Re < 100$, $1.1\times10^{-5} < Mo < 7$) was proposed based on the experimental data by *Raymond and Rosant* (2000) using the Reynolds number Re and the Weber number We [17]:

$$E = \frac{1 - \lambda_v We}{1 - \frac{1}{2}\lambda_v We} \tag{18}$$

$$\lambda_v = \frac{1}{12}\left(1 - \frac{3}{25}\frac{We}{Re}\right) \tag{19}$$

$$Re = \frac{d_e \rho_l u_t}{\mu_l} \tag{20}$$

Where μ_l respersent the viscosity of the liquid.

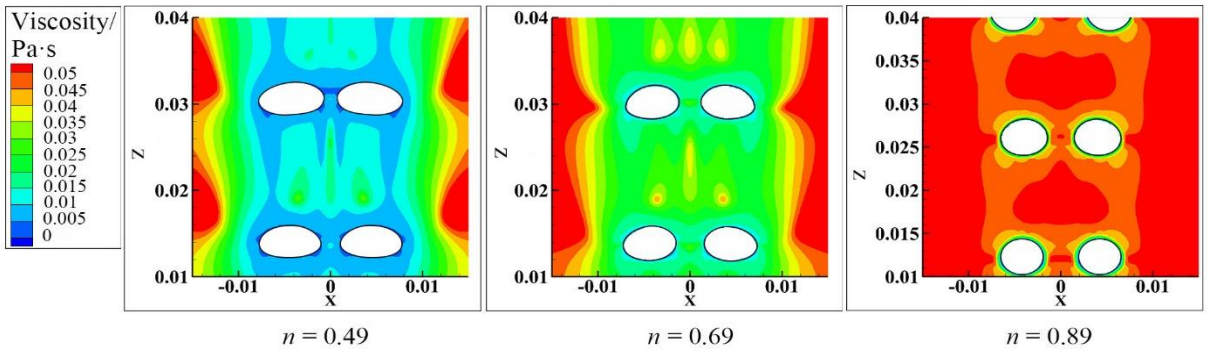

Fig. 11: The liquid viscosity around bubbles at t = 0.12 s and Y = - 0.0023 m. The black profile lines represent the interface location of bubbles, S* = 2.0, f = 16 Hz, K = 0.072 Pa·s^n.

Okawa et al. (2003) measured the deformation of the larger bubble rising in water (diameter: 0.6 ~ 3.5mm, $Eo < 1$), and correlated the aspect ratio E with the Eötvös number Eo as following [15]:

$$E = \frac{1}{1 + 1.97 Eo^{1.13}} \tag{21}$$

$$Eo = \frac{g d_e^2 \rho_l}{\sigma_l} \tag{22}$$

where g is the gravitational acceleration, d_e is the equivalent bubble diameter, ρ_l, σ_l are the density and surface tension of the liquid, respectively.

It was found by *Kelbaliyev and Ceylan* (2007) that small bubbles maintained their spherical shape, while larger ones achieved various shapes such as ellipsoidal, oblate ellipsoidal or spherical cap [24]. *Liu et al.* (2015) investigated the rising motion of a single bubble in stagnant water and glycerol aqueous solution by analyzing the wide experimental data [45]. According to the comparison and correction of available correlations in the literature, new correlations of aspect ratio E including Eötvös number Eo, Weber number We and Reynolds number Re for the bubble in water and glycerol aqueous solution were given as bellow, respectively:

$$E = \frac{1}{0.995 + 0.154 We^{1.705} Eo^{-0.405}} \quad \text{(for water)} \tag{23}$$

$$E = \frac{1}{0.991 + 0.115 We^{0.568} Re^{0.384}} \tag{24}$$

(for glycerol aqueous solution)

In terms of the shear thinning non-Newtonian fluids in the work, the Morton number Mo could be calcualted as follow:

$$Mo = \frac{g K^4 u_b^{4(n-1)}}{d_e^{4(n-1)} \sigma_l^3 \rho_l} \tag{25}$$

The comparison between the calculated results of models in the literature and the numerical values is shown in Fig. 12.

Fig. 12 shows an unsatisfactory deviation for these correlations in the literature with least difference for the model of *Liu et al.* (2015) [45]. As discussed in Sections 3.3~3.5, the bubble deformation for the multi-bubble system is more complex compared with the single bubble system, this could be attributed to the wake effect of leading bubbles and the hindrance of liquid to horizontal motion of bubbles, which are affected by the diameter, initial distance and formation frequency of the bubble as well as the liquid property. Therefore, the prediction model of the aspect ratio should consist of aforementioned factors for multi-bubble system in the shear thinning fluids. A correction factor $G(S,f)$, characterizing the influence of the wake effect and hindrance of liquid to horizontal motion of bubbles, was proposed to modify the model of *Liu et al.* (2015) for the bubble of the multi-bubble system in the shear-thinning fluids [45].

$$G(S,f) = \frac{E_s}{E_m} = 1 + a\left(S^*\right)^b \left(f^*\right)^c \tag{26}$$

$$S^* = \frac{S}{d_e} \tag{27}$$

$$f^* = \frac{1}{f \cdot t_{single}} \tag{28}$$

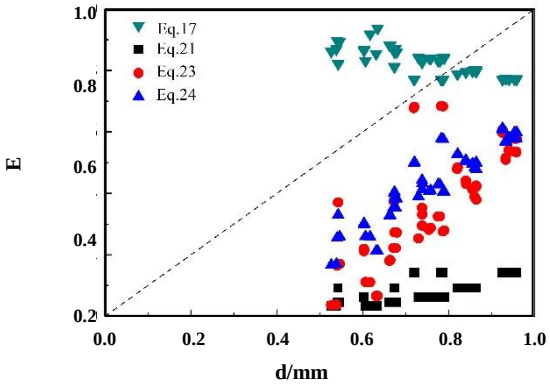

Fig. 12: Comparisons between calculated results and simulation values.

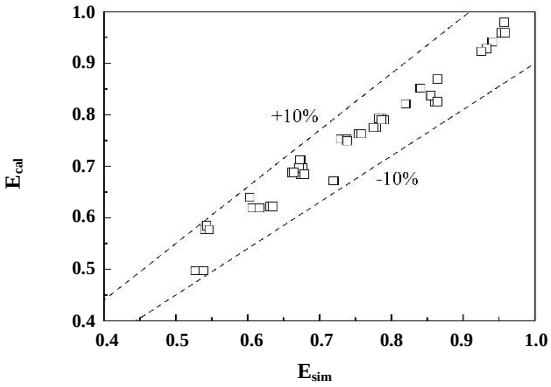

Fig. 13: Comparisons between prediction values and simulation results.

where S^* and f^* are the dimentionless distance and formation frequency of the bubble; d_e, S, f are the equivalent diameter, initial distance and formation frequency of the bubble; t_{single} is the time of the single bubble attained steady.

$$G(S,f)=\frac{E_s}{E_m}=1-0.15\left(S^*\right)^{0.71}\left(f^*\right)^{-0.40} \quad (29)$$

The modified model of *Liu et al.* (2015) for a single bubble in the shear-thinning fluids was obtained by fitting with the simulation results of the single bubble system under the identical operation [45].

$$E_s=\frac{1}{\left(1+0.064Re_s^{0.47}We_s^{0.28}\right)} \quad (30)$$

The final correlation of the aspect ratio of the bubble for the multi-bubble system in the shear thinning fluids was obtain:

$$E_m=\frac{E_s}{G(S,f)}= \quad (31)$$

$$\frac{1}{\left(1-0.15\left(S^*\right)^{0.71}\left(f^*\right)^{-0.40}\right)\left(1+0.064Re_s^{0.47}We_s^{0.28}\right)}$$

The comparison between calculated values by Eq. (31) and the simulation results is shown in Fig. 13, indicating a good predicting accuracy with average relative error 2.4%.

CONCLUSIONS

The focus of this study is the deformation of bubbles with equilateral triangle arrangement continuously rising in shear-thinning non-Newtonian fluids. The influences of bubble diameter, initial bubble distance, bubble formation frequency and liquid rheological property on the bubble deformation and aspect ratio were investigated for the multi-bubble systems and compared with a single bubble system.

It was found that the inertial force and viscous force on the bubble strengthens for the larger bubble, and their influences on bubbles would exceed that of the surface tension, leading to the bubble deforms from sphere to the ellipsoid or spherical cap. The influence factors of bubble deformation for the multi-bubble systems are more complicated compared with a free rising single bubble. For the continuously rising bubbles, the viscous force on the trailing bubble cluster declines while the inertial force enlarges due to the wake effect of the leading bubble cluster, resulting in a compression on the bubble in vertical direction. In addition, the liquid in the middle of bubbles hinders the approaching motion in radial direction, which leads to the radial shrinkage of bubbles. These influences finally result in higher aspect ratio of for the multi-bubble system than the single bubble system.

The simulation results of bubble deformation for the multi-bubble system were quantitative analysis and compared with models in the literature, showing large deviations. Therefore, a new correlation of the bubble aspect ratio for the multi-bubble systems in shear thinning non-Newtonian fluids was proposed based on the model of *Liu et al.* (2015) considering the influence of the wake effect and radial interaction [45]. The average deviation of the new correlation was 2.4%, showing a good agreement. These results would provide essential basis for the design and optimum of the multi-phase apparatus.

Acknowledgments

Supported by the National Nature Science Foundation of China (No. 91834303, 91434204).

Nomenclature

Notation:

U	Velocity vector, m/s
D	Stress tensor, N/m
F_s	Body force caused by surface tension, N/m
Q	Volume fraction function, dimensionless
G	Gravitational acceleration, m/s^2
K	Consistency coefficient, Pa·s^n
n	Flow index, dimensionless
n	Unit normal vector
E	Aspect ratio, dimensionless
d_v	Vertical bubble diameter, m
d_h	Horizontal projective bubble diameter, m
Re	Reynolds number, dimensionless
Eo	Eötvös number, dimensionless
Mo	Morton number, dimensionless
We	Weber number, dimensionless
Ta	Tadaki number, dimensionless
d_e	Equivalent bubble diameter, m
u_b	Bubble rising velocity, m/s
u_t	Bubble stable rising velocity, m/s
S	Initial bubble distance, m
f	Bubble formation frequency, Hz
S^*	Normalized bubble distance, dimensionless
f^*	Normalized bubble formation frequency, dimensionless
t_{single}	Time of the single bubble attained steady, s
a, *b*, *c*, *d*	Fitting parameters, dimensionless

Greek Letters

γ	Shear rate, s^{-1}
μ	Liquid viscosity, Pa·s
ρ	Density of liquid phase, kg/m^3
σ	Surface tension, N/m

Subscripts

g	Gas phase
l	Liquid phase
s	A single bubble
m	Multi bubbles

Received : Nov. 16, 2019 ; Accepted : Jan. 3, 2020

REFERENCES

[1] Davidson L., Erwin H., Amick J.R., Formation of Gas Bubbles at Horizontal Orifices, *AIChE J.*, **2**: 337-342 (1956).

[2] Miyahara T., Wang W.H., Takahashi T., Bubble Formation at a Submerged Orifice in Non-Newtonian and Highly Viscous Newtonian Liquids, *J. Chem. Eng. Jpn.(JCEJAQ)*, **21**: 620-626 (1988).

[3] Jin B., Yin P.H., Lant P., Hydrodynamics and Mass Transfer Coefficient in Three-Phase Air-Lift Reactors Containing Activated Sludge, *Chem. Eng. Process. (CENPEU)*, **45**: 608-617 (2006).

[4] Besagni G., Inzoli F., Bubble Size Distributions and Shapes in Annular Gap Bubble Column, *Exp. Therm. Fluid Sci. (ETFSEO)*, **74**: 27-48 (2016).

[5] Álvarez A., Sanjurjo B., Cancela A., Navaza J.M., Mass Transfer and Influence of Physical Properties of Solutions in a Bubble Column, *Chem. Eng. Res. Des. (CERDEE)*, **78**: 889-893 (2000).

[6] Ponoth S.S., McLaughlin J.B., Numerical Simulation of Mass Transfer for Bubbles in Water, *Chem. Eng. Sci. (CESCAC)*, **55**: 1237-1255 (2000).

[7] Hirt C.W., Nichols B.D., Volume of Fluid (VOF) Method for the Dynamics of Free Boundaries, *J. Comput. Phys. (JCTPAH)*, **39**: 201-225 (1981).

[8] Chen L., Li Y.G., Manasseh R., "The Coalescence of Bubbles-A Numerical Study", *Third International Conference on Multiphase Flow*, Lyon, France (1998).

[9] Wijngaarden L.V., The Mean Rise Velocity of Pairwise-Interacting Bubbles in Liquid, *J. Fluid Mech. (JFLSA)*, **251**: 55-78 (1993).

[10] Olmos E., Gentric C., Vial C., Wild G., Midoux N., Numerical Simulation of Multiphase Flow in Bubble Column Reactors. Influence of Bubble Coalescence and Break-Up, *Chem. Eng. Sci. (CESCAC)*, **56**: 6359-6365 (2001).

[11] Olmos E., Gentric C., Midoux N., Numerical Description of Flow Regime Transitions in Bubble Column Reactors by a Multiple Gas-Phase Model, *Chem. Eng. Sci. (CESCAC)*, **58**: 2113-2121 (2003).

[12] Baker G.R., Moore D.W., The Rise and Distortion of a Two-Dimensional Gas Bubble in an Inviscid Liquid, *Phys. Fluids (PHFLE)*, **1**: 1451-1459 (1989).

[13] Clift R., Grace J., Weber M., "Bubbles, Drops and Particles", Academic Press, New York (1978).

[14] Wellek R.M., Agrawal A.K., Skelland A.H.P., Shape of Liquid Drops Moving in Liquid Media, *AIChE J. (AICEAC)*, **12**: 854-862 (1966).

[15] Okawa T., Tanaka T., Kataoka I., Mori M., Temperature effect on Single Bubble Rise Characteristics in Stagnant Distilled Water, *Int. J. Heat Mass Transfer (IJHMAK)*, **6**: 903-913 (2003).

[16] Bhaga D., Weber M.E., Bubbles in Viscous Liquids Shapes Wakes and Velocities, *J. Fluid Mech. (JFLSA)*, **105**: 61-85 (1981).

[17] Raymond F., Rosant J.M., A Numerical and Experimental Study of the Terminal Velocity and Shape of Bubbles in Viscous Liquids, *Chem. Eng. Sci. (CESCAC)*, **55**: 943-955 (2000).

[18] Legendre D., Zenit R., Velez-Cordero J.R., On the Deformation of Gas Bubbles In Liquids, *Phys Fluids*, **24**: 1-13 (2012).

[19] Tripathi M.K., Sahu K.C., Karapetsas G., Matar O.K., Bubble Rise Dynamics in a Viscoplastic Material, *J. Non-Newtonian Fluid Mech. (JNFMDI)*, **222**: 217–226 (2015).

[20] Premlata A.R., Tripathi M.K, Karri B., Sahu K.C., Dynamics of an Air Bubble Rising in a Non-Newtonian Liquid in the Axisymmetric Regime, *J. Non-Newtonian Fluid Mech. (JNFMDI)*, **239**: 53–61 (2017).

[21] Xu X.F., Zhang J., Liu F.X., Wang X.J., Wei W., Liu Z.J., Rising Behavior of Single Bubble in Infinite Stagnant Non-Newtonian Liquids, *Int. J. Multiphase Flow (IJMFBP)*, **95**: 84-90 (2017).

[22] Pang M.J., Lu M.J., Numerical Study on Dynamics of Single Bubble Rising in Shear-Thinning Power-Law Fluid in Different Gravity Environment, *Vacuum*, **153**, 101-111 (2018).

[23] Moore D.W., The Rise of a Gas Bubble in a Viscous Liquid. *J. Fluid Mech. (JFLSA)*, **6**: 113-130 (1959).

[24] Kelbaliyev G., Ceylan K., Development of New Empirical Equations for Estimation of Drag Coefficient, Shape Deformation, and Rising Velocity of Gas Bubbles or Liquid Drops, *Chem. Eng. Commun. (CEGCAK)*, **194**: 1623-1637 (2007).

[25] Chen L., Garimella S.V., Reizes J.A., Leonardi E., The Development of a Bubble Rising in a Viscous Liquid, *J. Fluid Mech. (JFLSA)*, **387**: 61-96 (1999).

[26] Taylor T.D., Acrivos A., On the Deformation and Drag of a Falling Viscous Drop at Low Reynolds Number, *J. Fluid Mech. (JFLSA)*, **18**: 466-476 (1964).

[27] Celata G.P., Cumo M., D'Annibale F., Tomiyama A., The Wake Effect on Bubble Rising Velocity in One-Component Systems, *Int. J. Multiphase Flow (IJMFBP)*, **30**: 939-961 (2004).

[28] Lalanne B., Chebel N.A., Vejražka J., Tanguy S., Masbernat O., Risso F., Non-Linear Shape Oscillations of Rising Drops and Bubbles: Experiments and Simulations, *Phys. Fluids (PHFLE)*, **27**: 123305 (2015).

[29] Darmana D., Deen N.G., Kuipers J.A.M., Parallelization of an Euler-Lagrange Model Using Mixed Domain Decomposition and a Mirror Domain Technique: Application to Dispersed Gas-Liquid Two-Phase Flow, *J. Comput. Phys. (JCTPAH)*, **220**: 216-248 (2006).

[30] Lau Y.M., Bai W., Deenn N.G., Kuipers J.A.M., Numerical Study of Bubble Break-Up in Bubbly Flows Using a Deterministic Eule-Lagrange Framework, *Chem. Eng. Sci. (CESCAC)*, **108**: 9-22 (2014).

[31] Legendre D., Zevenhoven R., Detailed Experimental Study on the Dissolution Of CO_2 and Air Bubbles Rising in Water, *Chem. Eng. Sci. (CESCAC)*, **158**: 552-560 (2017).

[32] Waele A de., Viscometry and Plastometry. *J. Oil Colour Chem. Assoc. (JOCCAB)*, **6(38)**: 33-88 (1923).

[33] Brackbill J.U., Kothe D.B., Zemach C., A Continuum Method for Modeling Surface Tension, *J. Comput. Phys. (JCTPAH)*, **100**: 335-354 (1992).

[34] Guan X.P., Li Z.Q., Wang L.J., Cheng Y.W., Li X., CFD Simulation of Bubble Dynamics in Bubble Columns With Internals, *Ind. Eng. Chem. Res. (IECERD)*, **53**: 16529-16538 (2014).

[35] Georgoulas A., Koukouvinis P., Gavaises M., Marengo M., Numerical Investigation of Quasi-Static Bubble Growth and Detachment from Submerged Orifices in Isothermal Liquid Pools: The Effect of Varying Fluid Properties And Gravity Levels, *Int. J. Multiphase Flow (IJMFBP)*, **74**: 59-78 (2015).

[36] Feng J.J., Li X.C., Bao Y.Y., Cai Z.Q., Gao Z.M., Coalescence and Conjunction of Two In-Line Bubbles at Low Reynolds Numbers, *Chem. Eng. Sci. (CESCAC)*, **141**: 261-270 (2016).

[37] Sun W.P., Zhu C.Y., Fu T.T., Yang H., Ma Y.G., Li H.Z., The Minimum in-Line Coalescence Height of Bubbles in Non-Newtonian Fluid, *Int. J. Multiphase Flow (IJMFBP)*, **92**: 161-170 (2017).

[38] Moore D.W., The Velocity of Rising of Distorted Gas Bubbles in a Liquid of Small Viscosity, *J. Fluid Mech. (JFLSA)*, **23**: 749-766 (1965).

[39] Bozzano G., Dente M., Shape and Terminal Velocity of Single Bubble Motion a Novel Approach, *Comput. Chem. Eng. (CCENDW)*, **25**: 571-576 (2001).

[40] Wu M.M., Gharib M., Experimental Studies on the Shape and Path of Small Air Bubbles Rising in Clean Water, *Phys. Fluids (PHFLE)*, **14**: 49-52 (2002).

[41] Katz J., Meneveau C., Wake-Induced Relative Motion of Bubbles Rising in Line, *Int. J. Multiphase Flow (IJMFBP)*, **22**: 239-258 (1996).

[42] Wijngaarden L.V., Hydrodynamic Interaction Between Gas Bubbles in Liquid, *J. Fluid Mech. (JFLSA)*, **77(1)**: 27-44 (1976).

[43] Biesheuvel A., Wijngaarden L.V., The Motion of Pairs of Gas Bubbles in A Perfect Liquid, *J. Eng. Math (JLEMAU).*, **16(4)**: 349-365 (1982).

[44] Fan L.S., Tsuchiya K., "Bubble Wake Dynamics in Liquids and Liquid-Solid Suspensions", Butterworth Heinemann, Oxford (1990).

[45] Liu L., Yan H.J., Zhao G.J., Experimental Studies on the Shape and Motion of Air Bubbles in Viscous Liquids, *Exp. Therm. Fluid Sci. (ETFSEO)*, **62**: 109-121 (2015).

[46] Lane C.D., Parisien V., Macchi A., Donaldson A.A., Investigation of Bubble Swarm Drag at Elevated Pressure in a Contaminated System, *Chem. Eng. Sci. (CESCAC)*, **152**: 381-391 (2016).

[47] Tadaki T., Maeda S., On the Shape and Velocity of Single Air Bubbles Rising in Various Liquids, *Kagaku Kogaku (KKGKA)*, **25**: 254-264 (1961).

[48] Vakhrushev I.A., Efremov G.I., The Velocities of Single Gas Bubbles in Liquids, *Chem. Technol. Fuels Oils (CTFOAK)*, **5**: 376-379 (1970).